# A Study on Voltage Stability Improvement by the Efficient Network Reconfiguration Algorithm

Byung-Seop Kim*, Joong-Rin Shin**, Jong-Bae Park** and Yong-Hak Shin*

**Abstract** - This paper presents an optimal routing algorithm (ORA) for maximizing voltage stability as well as for minimizing power loss in radial power systems. In the proposed ORA, a novel voltage stability index (VSI) for real-time assessment is newly introduced based on the conventional critical transmission path framework. In addition, the suggested algorithm can automatically detect the critical transmission paths resulting in voltage collapse when additional real or reactive loads are added. To implement an effective ORA, we have developed an improved branch exchange (IBE) method based on a loss calculation index and tie-branch power flow equations, which are suggested for real-time applications. The proposed algorithm has been tested with IEEE test systems as well as a large-scale power system in Korea to demonstrate its effectiveness and efficiency.

**Keywords:** Branch exchange, Combinatorial optimization, Loss minimization, Optimal routing algorithm, Radial power system, Voltage stability index

## 1. Introduction

There has been a growing interest in the optimal operation of radial networks during the past few decades, particularly in the area of distribution system automation, all to increase economics as well as security. Some transmission systems as well as distribution systems are operated in a radial network structure. Therefore, modifying the topological structures of the radial power systems from time to time by changing the open/closed states of the sectionalizing and tie switches to transfer loads from one transmission path to another, can significantly improve the operation conditions of the power systems. If the loads are more efficiently rescheduled by a suitable ORA, the voltage stability in a system can be enhanced and power loss can be reduced as well along the transmission paths. Recently, several analytical techniques for real-world applications have been proposed to assess the risk of voltage instability in radial power systems [1, 2].

Voltage stability is a very important issue in power system operations and planning since voltage instability may lead to voltage collapse and possibly a total system black out [3]. Voltage instability can occur when a power system is heavily loaded in the transmission lines and/or insufficiently supplied by the local reactive power

resources [5, 6]. Although the voltage stability problem is in its nature a dynamic one, a greater part of the researches have been devoted to the application of static methods for real-time applications. A Thevenin equivalent circuit framework is applied by Lachs *et. al.* to study voltage collapse phenomenon at a load bus [5]. The intimate relationship between voltage stability and power loss has been tackled in [4].

In this paper, a new optimal routing algorithm (ORA) not only to improve the voltage stability but also to reduce the power loss in radial power systems is developed. The suggested algorithm can efficiently perform rapid assessment of the voltage stability margin when the open/closed states of the sectionalizing and tie switches are changed. The problem has been formulated as a combinatorial optimization one, in which its objective function is the maximization of a newly devised voltage stability index (VSI) basically inspired by the conventional approach [7]. Additionally, in the proposed ORA, we have improved the conventional branch exchange method to reduce calculation burdens. The suggested improved branch exchange (IBE) method is implemented based on a new loss calculation index (LCI) and a tie branch power flow (TBP) equation to assess the impact on power loss due to the branch exchange in an analytical manner. The proposed ORA is resolved by genetic algorithm (GA) [13] to overcome the local optimum traps existing in the conventional branch exchange method. The proposed algorithm has been evaluated with the IEEE 32-bus, IEEE 69-bus systems [11, 12], and the 148-bus system of the

## 2. Problem Formulation

In general, the network reconfiguration problem in a radial power system is to find the configuration with the minimum power loss while the system constraints are satisfied [11]. However, in this paper, the optimal routing problem is formulated as a network reconfiguration problem that can result in voltage stability enhancement as well as loss minimization. Therefore, the base network for an optimal routing problem starts from a simple radial network with series impedances of $\bar{Z}_i = r_i + jx_i$, constant demands of $\bar{S}_{Di} = P_{Di} + Q_{Di}$, and a complex power flow of $\bar{S}_i = P_i + jQ_i$ as shown in Fig. 1.

Due to a large number of switching combinations during the branch exchange processes, the optimal routing problem is usually characterized as a combinatorial optimization problem. In this paper, the objective function and the corresponding constraints are formulated as follows, which is also considered as a combinatorial optimization problem.

$$\max_{X \in \Omega} VSI(X) \quad (1)$$

s.t

$$G_E(X) = 0$$

$$\bar{S}_i \le \bar{S}_i^{\max}, \quad i = 1, \cdots, N_B$$

where,

$$X = \{(\bar{S}_i, \bar{V}_i) \mid i = 1, \cdots, N_B\},$$

$$\Omega = \{X^* \mid L(X^*) \le L(X), \ G_R(X^*) = 0, X \in \Lambda\},$$

$$\Lambda = \{X_i \mid i = 1, \cdots, N_T\},$$

$VSI(\cdot)$: voltage stability index function,

$L(\cdot)$: real power loss function of a network configuration,

$G_E(\cdot)$: equality constraint of power balance equations,

$G_R(\cdot)$: equality constraint of a radial network configuration,

$\bar{V}_i, V_i$: voltage phasor and magnitude at bus $i$,

$r_i$: resistance of a branch connected with bus $i$,

$\bar{S}_i = P_i + jQ_i$: complex power flow at bus $i$,

$\bar{S}_i^{\max}$: complex power limits at bus $i$.

The real power loss function (*i.e.*, $L(\cdot)$) and the equality constraint of a radial network configuration (*i.e.*, $G_R(\cdot)$) in (1) are described in details as follows:

$$L(X) = \sum_{i \in N_B} (r_i \mid S_i \mid^2 / V_i^2)$$

$$G_R(X) = \left(N_B - \frac{1}{2}\sum_i^{TN}\sum_j^{TN} n_{ij}\right) + \left(\sum_i^{TN}(1 - B_i)\right) + \left(\sum_i^{TN}\sum_{\substack{j \neq i \\ p}}^{TN} n_{ij} n_{ip}\right) \quad (2)$$

where,

$$n_{ij} = \begin{cases} 1 & \text{if bus } i \text{ and bus } j \text{ are connected with together} \\ 0 & \text{otherwise} \end{cases}$$

$$B_i = \begin{cases} 1 & \text{if } \sum_i^{TN}\sum_j^{TN} n_{ij} \neq 0 \\ 0 & \text{otherwise} \end{cases}$$

In (1) and (2), $N_T$ signifies the total number of feasible network configurations to be composed during the branch exchange processes, and $N_B$ corresponds to the number of load buses except for the supply bus. Also, *TN* denotes the number of total buses. Additionally, *p* means a set of buses directly connected with both bus $i$ and bus $j$.
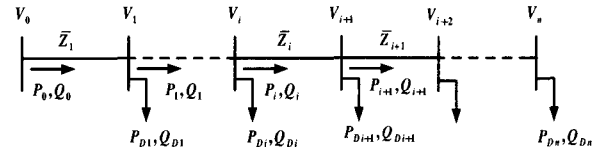


**Fig. 1** One-line diagram of a radial network.

## 3. Formulation of Voltage Stability Index

### 3.1 Critical Transmission Path

A radial transmission path with $n$ buses incurs line loss due to real and reactive loads. The loads at intermediate buses cause voltage drops along the paths. The key idea of the critical transmission path (CTP) is to project the voltage drop phasor at bus $n$ into the voltage phasor of the supply bus [7]. Therefore, the CTP can be defined as a series of buses with declining voltage magnitude, and the critical bus (*e.g.*, the end bus in the CTP) can be faced with voltage collapse when additional real or reactive loadings are required. In this paper, the idea of CTP has been partly adopted for voltage stability assessment in a general radial network system.

### 3.2 Derivation of Voltage Stability Index

The newly introduced voltage stability index (VSI) can be derived from a sample power system with two buses as

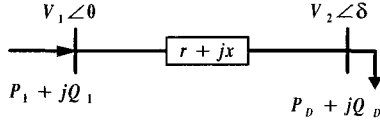shown in Fig. 2 and can be expanded to a $n$-bus power system without loss of generality.



**Fig. 2** Diagram of a power system with two buses.

The proposition has been started from the formulation of the system Jacobian matrix [$J$]. If we consider bus $I$ as the slack bus, the condition of the singularity can be derived from the determinant of the Jacobian matrix. Since the Jacobian matrix contains the state information of a network, a critical operation point can be defined from its singularity condition. From the power equation, the singularity condition can be derived as (3).

$$Det \ \mathbf{J} = \frac{\partial P_2}{\partial \delta} \frac{\partial Q_2}{\partial V_2} - \frac{\partial P_2}{\partial V_2} \frac{\partial Q_2}{\partial \delta} = 0 \tag{3}$$

The singularity condition of (3) can be finally arranged as the following compact form, which is induced in Appendix A.

$$2V_2 \cos \delta = V_1 \tag{4}$$

The derived (4) can be equivalently redefined as the function of projected direct axis component, $\Delta V_d$, in the phasor diagram of the two-bus system as illustrated in Fig. 3.
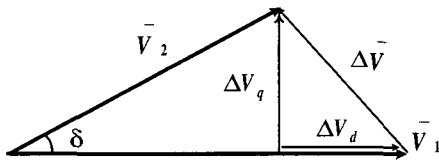


**Fig. 3** Voltage phasor diagram of a power system with two buses.

By Fig. 3, the singularity condition of (4) can be equivalently replaced by the projected direct axis component of the voltage drop phasor as (5):

$$0.5V_1 = \Delta V_d \tag{5}$$

The projected direct axis component in (5) is converted into equal power and impedance for applying the proposed ORA. The voltage drop phasor in Fig. 3 can be expressed in a rectangular form as follows:

$$\Delta \overline{V} = \Delta V_d + j\Delta V_q \tag{6}$$

Additionally, the relationship between the voltage drop phasor and voltage phasor in each bus, injected power, and impedance of the two-bus system is described as follows:

$$\Delta \overline{V} = (r + jx)(P_1 - jQ_1)/\overline{V}_1^* \tag{7}$$

Therefore, the projected direct axis component in (5) can be replaced by the actual part of (7). Therefore, we can obtain the voltage stability assessment information in the two-bus system as follows:

$$0.5V_1 = (P_1 r + Q_1 x)/V_1 \tag{8}$$

For the general expression of (8), we should expand it as a generic mathematical form with a $n$-bus system. Consequently, the voltage stability index with $n$ buses can be generalized as follows:

$$VSI = 0.5V_1 - (P_{eq} r_{eq} + Q_{eq} x_{eq})/V_1 \tag{9}$$

where,

$$P_{eq} = \sum (P_{Li}^{CTP} + P_{Di}^{CTP}), \quad Q_{eq} = \sum (Q_{Li}^{CTP} + Q_{Di}^{CTP}),$$

$$r_{eq} = \sum P_{Li}^{CTP} /(P_{eq}^2 + Q_{eq}^2), \quad x_{eq} = \sum Q_{Li}^{CTP} /(P_{eq}^2 + Q_{eq}^2).$$

The equivalent impedance in (9) is described in Appendix B. Here, $(\cdot)_{Li}^{CTP}$ and $(\cdot)_{Di}^{CTP}$ imply the power loss and power load of branch (i) along the CTP. When this index approaches zero value, the power transfer on the critical transmission path becomes unstable due to the voltage collapse.

## 4. Improved Branch Exchange Method

The branch exchange operation is initially introduced to represent a switching option by closing a single tie switch and opening a single sectionalizing switch to preserve the radiality of the feeders [10]. Recently, Baran and Wu [11] have developed an effective loss reduction formula. However, Baran's method requires a relatively long computation time to identify the branches to be exchanged since it considers every switching exchange in a loop network at each search level and calculates the loss change for each selected switching set using the load flow analysis. Therefore, in this paper, an improved branch exchange (IBE) method for the ORA has been developed to overcome the aforementioned dimensionality problem as

well as the calculation burden inherent in the studies.

## 4.1 Formulation of Tie Branch Power Equation

If a load on one side of the tie branch is transferred to the other side due to branch exchange, the new power flow along the closed tie branch will be enacted. The main purpose of a tie branch power flow (TBP) equation is to directly calculate the changed power flow along the closed tie branch without iterative load flow analysis. After the occurrence of a branch exchange, which is performed by closing a single tie switch and opening a single sectionalizing switch, in the L-side, a new power flow, $P_t + jQ_t$, will be generated as illustrated in Fig. 4. In Fig. 4, the branch (t') denotes a closed tie branch and the load, $P_{Dt} + jQ_{Dt}$, signifies a transferred load from the L-side to the R-side due to the branch exchange.
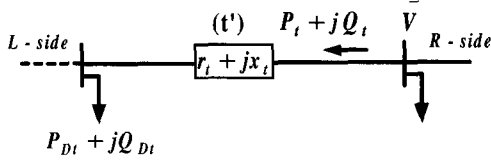


**Fig. 4** Two-bus system diagram connected with a tie branch (t').

The formulation for the TBP equation can be initiated from the general power balance equation of a closed tie branch (t') as follows:

$$P_t + jQ_t = (r_t + jx_t)\frac{|P_t + jQ_t|^2}{V^2} + P_{Dt} + jQ_{Dt} \qquad (10)$$

From (10), after classifying the real and imaginary parts, a set of quadratic equations in terms of the power flow are derived as follows:

$$(r_t^2 + x_t^2)P_t^2 - (2x_t^2 P_{Dt} - 2r_t x_t Q_{Dt} + V^2 r_t)P_t$$
$$+ (x_t^2 P_{Dt}^2 + r_t^2 Q_{Dt}^2 - 2r_t x_t P_{Dt}Q_{Dt} + V^2 r_t P_{Dt}) = 0$$
$$(r_t^2 + x_t^2)Q_t^2 - (2x_t^2 Q_{Dt} - 2r_t x_t P_{Dt} + V^2 x_t)Q_t$$
$$+ (x_t^2 P_{Dt}^2 + r_t^2 Q_{Dt}^2 - 2r_t x_t P_{Dt}Q_{Dt} + V^2 x_t Q_{Dt}) = 0$$

$$(11)$$

(11) has the quadratic form and one can find the real roots of the real and reactive power flow equations, respectively as in (12).

$$P_t = \frac{K_p - \sqrt{K_p^2 - 4K_z(x_t P_{Dt} - r_t Q_{Dt})^2 - 4K_z V^2 r_t P_{Dt}}}{2K_z}$$

$$(12)$$

$$Q_t = \frac{K_q - \sqrt{K_q^2 - 4K_z(x_t P_{Dt} - r_t Q_{Dt})^2 - 4K_z V^2 x_t Q_{Dt}}}{2K_z}$$

where,

$$K_p = 2x_t^2 P_{Dt} - 2r_t x_t Q_{Dt} + V^2 r_t ,$$

$$K_q = 2r_t^2 Q_{Dt} - 2r_t x_t P_{Dt} + V^2 x_t ,$$

$$K_z = r_t^2 + x_t^2 .$$

In this paper, especially, we use the estimated TBP equation by substituting $V^2$ for $\tilde{V}^2$ in the equation. The estimated TBP equation can be effectively used as a method to exclude iterative load flow calculations during branch exchanges in a loop network system. The approximate voltage square, $\tilde{V}^2$, indicates a value obtained by the load flow calculation in the previous search level. Implicit function forms of the estimation can be expressed as follows:

$$\hat{P}_t = P(r_t, x_t, P_{Dt}, Q_{Dt}, \tilde{V}^2)$$
$$\hat{Q}_t = Q(r_t, x_t, P_{Dt}, Q_{Dt}, \tilde{V}^2)$$

$$(13)$$

## 4.2 Selection of Optimum Branch via Loss Calculation Index

In this section, a new loss calculation index (LCI) is suggested to find the optimum branch to be exchanged. The proposed index, which is based on the TBP equation, can be applied to either the higher voltage side or the lower voltage side in a loop network. Therefore, we can divide a loop network into L-side and R-side, where the former implies the part of decreasing power loss and the latter implies the part of increasing power loss, respectively. If a loop network is selected as the optimum loop, the variations of real power loss due to branch exchange (BE) between branch (t) and branch (t,con) are expressed as (14). The subscript, *t,con*, implies the number of adjacent branches, which are directly connected to the tie branch before a branch exchange operation. In (14), the change of real power loss due to a branch exchange between branch (t) and branch (t,con) is expressed as a sum of a real part loss, $\Delta P_{loss}$, and a reactive part loss, $\Delta Q_{loss}$. This index is also explained in Appendix C.

$$\Delta LCI_{t,con} = \Delta P_{loss}(S) + \Delta Q_{loss}(T) \qquad (14)$$

where,

$$S = \left[ r_t , P_i , \hat{P}_t , P_{t,con} , P_{Dt} \right]^T,$$

$$T = \left[ r_t , Q_i , \hat{Q}_t , Q_{t,con} , Q_{Dt} \right]^T.$$

Here, $P_i$ and $Q_i$ denote real and reactive power flow in branch (i) before a BE, respectively, and $P_{t,con}$ and $Q_{t,con}$ imply real and reactive power flow in branch (t,con) before a BE, respectively.

## 5. Solution Procedure

The solution procedure for the optimal routing problem is described in Fig. 5. In the flowchart, the Distflow method [12] is adopted as a load flow analysis tool. In Fig. 5, the proposed loss index module is carried out by the following steps;

Step (a) Calculate $\Delta LCI$ due to the BE between the current tie and its adjacent branch in all loop networks.

Step (b) Determine the highest $\Delta LCI$ as a temporary optimum loop network in the present search level.

Step (c) Perform a BE between (t) and (t,con) for the temporary optimum loop network.

Step (d) Calculate $\hat{P}_t$, $\hat{Q}_t$.

Step (e) Calculate $\Delta P_{loss}(S)$, $\Delta Q_{loss}(T)$, and $\Delta LCI_{t,con}$.

Step (f) If all branches in the tentative optimum loop are considered, select the best candidate satisfying the constraints, otherwise go to step (c).
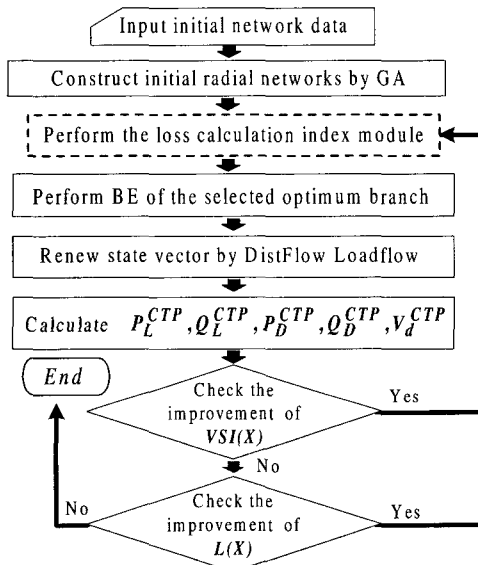


**Fig. 5** Solution procedure of the proposed algorithm.

## 6. Case Studies and Discussions

The suggested framework is tested with the IEEE 32-bus and IEEE 69-bus radial power systems [11, 12] and the 148-bus power system [15] of the Korea Electric Power Corporation (KEPCO). The ULTC action is blocked and the loads are considered to be constant power ones. The algorithm is implemented in a Pentium-400MHz IBM compatible PC. In the following tables and figures, the standard units are second (sec.), per unit (p.u.), kW, and kVar, respectively. Table 1 shows the brief summary of the test systems.

**Table 1** Summary of Test Systems

| Test Systems | No. of Buses | No. of Branches | No. of Loop Networks | Total Demand |
|---|---|---|---|---|
| 32 Bus | 33 | 37 | 5 | 3715 + j2300 |
| 69 Bus | 70 | 74 | 5 | 3802.2 + j2694.6 |
| 148 Bus | 149 | 167 | 19 | 44292.8 + j21510.7 |

### 6.1 VSI Assessment Results

Table 2 illustrates the obtained results of the CTP of the 148-bus KEPCO system, which are obtained by the proposed algorithm. In Table 2, we can observe that the buses along the CTP are composed of the descending orders of the bus voltage magnitude. In Table 2, $\Sigma\, S_{D,CTP}$ and $\Sigma\, S_{L,CTP}$ denote the complex power load and complex power loss along the CTP and the critical voltage and $V^{cr}$, indicates the voltage of the last load bus in the CTP.

Table 3 shows the comparison of the voltage stability index between the proposed VSI and the conventional VSI (JVSI) [9] on the 69-bus system. Although both results have shown similar transitions, the proposed VSI has provided very reliable results. For example, when the critical voltage was 0.599 in the case of the loading rate by 3 times, the values of VSI and JVSI are 0.011 and 0.737, respectively. This means that the margins to reach the voltage collapse are 1.1% in VSI and 26.3% in JVSI, respectively. These results indicate that the proposed VSI can effectively detect regional information on voltage collapse compared with the JVSI.

Fig. 6 shows the VSI curve of the 69-bus system. In this case, the open/closed statuses of all switches are equally maintained in the initial network. The loadings of all buses are simultaneously increased by the ratio of S/S-base where S-base is set as the total complex load in the initial network. When S/S-base becomes 3.07, the VSI, the detected critical bus, and the critical voltage are 0.041, 54, and 0.6014, respectively. Also, the CTP is composed of 0, 1, 2, 2e, 3, 4, 5, 6, 7, 8, 42, 43, 44, 45, 46, 47, 48, 49, 50, 51, 52, 53, and 54 buses. If we apply the Newton-Rapshon

load flow method, it diverges when the S/S-base has reached 2.5 where the corresponding VSI and the critical voltage are only 0.32236 and 0.719, respectively.

**Table 2** Results of The CTP of The 148-Bus System

| Bus No. | Vol. | Bus No. | Vol. | Bus No. | Vol. | Bus No. | Vol. | Bus No. | Vol. |
|---------|------|---------|------|---------|------|---------|------|---------|------|
| 0 | 1.000 | 34 | 0.970 | 68 | 0.963 | 102 | 0.974 | 136 | 0.975 |
| 1 | 1.000 | 35 | 0.966 | 69 | 0.973 | 103 | 0.974 | 137 | 0.968 |
| 2 | 1.000 | 36 | 0.976 | 70 | 0.974 | 104 | 0.973 | 138 | 0.952 |
| 3 | 1.000 | 37 | 0.975 | 71 | 0.970 | 105 | 0.973 | 139 | 0.954 |
| 4 | 1.000 | 38 | 0.975 | 72 | 0.972 | 106 | 0.971 | 140 | 0.973 |
| 5 | 1.000 | 39 | 0.972 | 73 | 0.972 | 107 | 0.968 | 141 | 0.973 |
| 6 | 1.000 | 40 | 0.972 | 74 | 0.971 | 108 | 0.961 | 142 | 0.975 |
| 7 | 1.000 | 41 | 0.972 | 75 | 0.969 | 109 | 0.970 | 143 | 0.968 |
| 8 | 0.989 | 42 | 0.972 | 76 | 0.970 | 110 | 0.975 | 144 | 0.973 |
| 9 | 0.977 | 43 | 0.971 | 77 | 0.970 | 111 | 0.975 | 145 | 0.973 |
| 10 | 0.976 | 44 | 0.970 | 78 | 0.970 | 112 | 0.975 | 146 | 0.973 |
| 11 | 0.971 | 45 | 0.970 | 79 | 0.973 | 113 | 0.971 | 147 | 0.974 |
| 12 | 0.979 | 46 | 0.970 | 80 | 0.974 | 114 | 0.968 | 148 | 0.973 |
| 13 | 0.976 | 47 | 0.966 | 81 | 0.974 | 115 | 0.960 | | |
| 14 | 0.973 | 48 | 0.975 | 82 | 0.970 | 116 | 0.972 | | |
| 15 | 0.976 | 49 | 0.974 | 83 | 0.973 | 117 | 0.970 | | |
| 16 | 0.971 | 50 | 0.973 | 84 | 0.972 | 118 | 0.975 | | |
| 17 | 0.970 | 51 | 0.971 | 85 | 0.968 | 119 | 0.975 | | |
| 18 | 0.978 | 52 | 0.972 | 86 | 0.970 | 120 | 0.971 | | |
| 19 | 0.977 | 53 | 0.972 | 87 | 0.970 | 121 | 0.968 | | |
| 20 | 0.976 | 54 | 0.969 | 88 | 0.970 | 122 | 0.955 | | |
| 21 | 0.972 | 55 | 0.970 | 89 | 0.972 | 123 | 0.960 | | |
| 22 | 0.971 | 56 | 0.971 | 90 | 0.975 | 124 | 0.972 | | |
| 23 | 0.976 | 57 | 0.970 | 91 | 0.974 | 125 | 0.970 | | |
| 24 | 0.971 | 58 | 0.964 | 92 | 0.974 | 126 | 0.970 | | |
| 25 | 0.971 | 59 | 0.974 | 93 | 0.973 | 127 | 0.975 | | |
| 26 | 0.968 | 60 | 0.975 | 94 | 0.973 | 128 | 0.968 | | |
| 27 | 0.976 | 61 | 0.971 | 95 | 0.971 | 129 | 0.954 | | |
| 28 | 0.976 | 62 | 0.972 | 96 | 0.968 | 130 | 0.960 | | |
| 29 | 0.976 | 63 | 0.972 | 97 | 0.968 | 131 | 0.960 | | |
| 30 | 0.972 | 64 | 0.970 | 98 | 0.962 | 132 | 0.972 | | |
| 31 | 0.972 | 65 | 0.970 | 99 | 0.971 | 133 | 0.973 | | |
| 32 | 0.971 | 66 | 0.970 | 100 | 0.975 | 134 | 0.970 | | |
| 33 | 0.971 | 67 | 0.970 | 101 | 0.975 | 135 | 0.970 | | |
| CTP | 0, 1, 3, 7, 11, 17, 26, 35, 47, 58, 68, 98, 108, 115, 122, 129, 138 | | | | | | | | |
| VSI | 0.45796 | $\Sigma\ S_{D,CTP}$ | | 8271.850 + j4003.476 | | | | | |
| $V^{cr}$ | 0.95220 | $\Sigma\ S_{L,CTP}$ | | 301.763 + j540.238 | | | | | |

**Table 3** Comparison of Voltage Stability Indexes in The 69-Bus System

| Loading rate (1 time) | | | | Loading rate (3 times) | | | |
|-----------------------|---------|------|------|------------------------|---------|------|------|
| Power loss | Critical voltage | VSI | JVSI | Power loss | Critical voltage | VSI | JVSI |
| 225.00 | 0.909 | 0.384 | 0.188 | 4165.49 | 0.599 | 0.011 | 0.737 |
| 138.94 | 0.925 | 0.449 | 0.160 | 1824.94 | 0.723 | 0.309 | 0.538 |
| 128.27 | 0.925 | 0.449 | 0.153 | 1716.20 | 0.741 | 0.322 | 0.512 |
| 123.04 | 0.926 | 0.452 | 0.147 | 1664.69 | 0.741 | 0.322 | 0.507 |
| 100.76 | 0.941 | 0.462 | 0.121 | 1645.19 | 0.741 | 0.322 | 0.503 |
| 100.68 | 0.941 | 0.462 | 0.121 | 1363.49 | 0.794 | 0.362 | 0.424 |
| 100.68 | 0.941 | 0.462 | 0.121 | 1278.01 | 0.794 | 0.363 | 0.426 |
| 100.68 | 0.941 | 0.462 | 0.121 | 1251.86 | 0.794 | 0.362 | 0.405 |
| 99.621 | 0.943 | 0.463 | 0.119 | 1251.31 | 0.794 | 0.362 | 0.405 |
| | | | | 1217.67 | 0.794 | 0.362 | 0.407 |
| | | | | 1191.75 | 0.794 | 0.362 | 0.401 |
| | | | | 1190.39 | 0.794 | 0.362 | 0.401 |
| | | | | 1165.23 | 0.800 | 0.367 | 0.393 |
| | | | | 1162.46 | 0.800 | 0.367 | 0.392 |
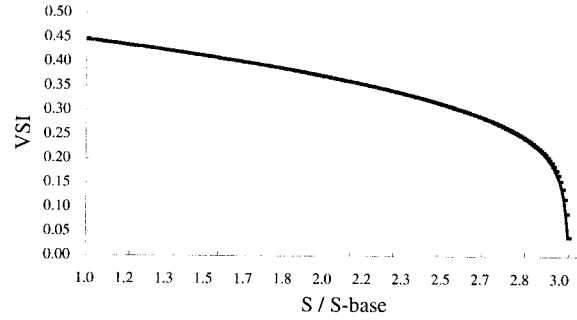


**Fig. 6** VSI curve of the 69-bus system.

## 6.2 Results of the IBE Method

Table 4 shows the obtained results from the TBP equation when real power loadings are sequentially increased. In Table 4, case 1 denotes the results obtained by the load flow analysis, which are considered as the reference case for comparisons. Case 2 denotes the results from the derived TBP equation of (12). From the results of case 2, we can see that the derived TBP is perfectly correct (*i.e.*, all error rates are 0%). Case 3 shows the results obtained when the approximated voltage in (13) is applied. In case 3, errors at higher voltage levels over 0.9 are

**Table 4** Examinations of The TBP Equation for The 69-Bus System

| Load flow analysis (case 1) | | |
|---|---|---|
| Real power loading (rate) | Branch power flow | |
| | Voltage | Real power flow |
| 280 (base) | 0.992 | 281.958 |
| 1400 (5 times) | 0.957 | 1435.803 |
| 2800 (10 times) | 0.907 | 2967.961 |
| 4200 (15 times) | 0.845 | 4680.618 |
| 5880 (21 times) | 0.721 | 7659.434 |
| TBP with voltage considered (case 2) | | |
| Voltage | Real power flow | Error rate (%) |
| 0.992 | 281.958 | 0.000 |
| 0.957 | 1435.803 | 0.000 |
| 0.907 | 2967.961 | 0.000 |
| 0.845 | 4680.618 | 0.000 |
| 0.721 | 7659.433 | 0.000 |
| TBP with voltage estimated (case 3) | | |
| Voltage | Real power flow | Error rate (%) |
| 0.992 | 281.958 | 0.000 |
| 0.966 | 1433.246 | 0.178 |
| 0.917 | 2963.591 | 0.147 |
| 0.859 | 4661.584 | 0.407 |
| 0.733 | 7551.397 | 1.411 |
| TBP with voltage neglected (case 4) | | |
| Voltage | Real power flow | Error rate (%) |
| 1.000 | 281.937 | 0.007 |
| 1.000 | 1432.684 | 0.217 |
| 1.000 | 2935.100 | 1.107 |
| 1.000 | 4519.815 | 3.436 |
| 1.000 | 6552.484 | 14.452 |

ignorable (e.g., 0.147% at 0.917 and 10 times loading), which indicates that the TBP equation can be used in estimating the new tie power flow during a BE. At the lower voltage levels, error rates are below 1.5% (e.g., 1.411% at 0.7337). These results show that the TBP equation of (13) can effectively replace the conventional load flow analysis in a practical sense and can dramatically reduce the computation time. In case 4, the voltage magnitude is considered as a constant and the error rates are relatively large when compared with case 3.

Table 5 and Table 6 show the comparisons between the proposed IBE method and Baran's method [11] in terms of the average computation time and the convergence probabilities. The results are based on the average values from one hundred trials. Especially, in these case studies, an initial radial network of Baran's method is determined through a random creation, on the other hand, the proposed IBE method is configured through the GA method [13].

**Table 5** Comparisons of Convergence Probabilities

| Optimization method | 32 bus | 69 bus | 148 bus |
|---|---|---|---|
| Baran method with initial network by random function | 91.32[%] | 87.23[%] | 75.09[%] |
| Proposed IBE method with GA | 100 [%] | 99.51[%] | 90.52[%] |

**Table 6** Comparisons of Average Computation Time

| Test systems | | Iteration number | No. of load flow calculation | Computation time [sec] |
|---|---|---|---|---|
| 32 Bus | [11] | 5 | 26 | 6.006 |
| | Pro. | 8 | 9 | 2.311 |
| 69 Bus | [11] | 5 | 26 | 8.611 |
| | Pro. | 9 | 10 | 3.681 |
| 148 Bus | [11] | 16 | 457 | 448.71 |
| | Pro. | 29 | 30 | 36.825 |

- Pro. : Proposed method.

## 6.3 Results of the ORA

Table 7 provides comparisons between the proposed IBE method and the conventional studies to show the reliability of the proposed algorithm. Table 8 demonstrates the convergence characteristics of the VSI and power loss in the IEEE 69-bus system. Fig. 7 also illustrates the convergence characteristics of the KEPCO 148-bus system. In the 69-bus system, the VSI has increased from 0.38409 to 0.46349 (i.e., VSI and loss improved 20.41% and 55.72%, respectively). In the 148-bus system, the VSI increased from 0.3316 to 0.4580 as well (i.e., VSI and loss improved 38.11% and 61.19%, respectively) due to the application of the suggested ORA.

**Table 7** Comparisons of BE Methods

| Test system | | Tie branch number (sending bus, receiving bus) | Power loss |
|---|---|---|---|
| 32 | [11] | 7(6,7), 9(8,9), 14(13, 14), 32(31,32), 37(24,28) | 139.549 |
| | Pro. | 7(6,7), 9(8,9), 14(13, 14), 32(31,32), 37(24,28) | 139.549 |
| 69 | [14] | 15(13,14), 59(47,48), 62(50, 51), 70(10, 70), 71(12,20) | 99.66 |
| | Pro. | 15(13,14), 58(46,47), 62(50, 51), 70(10, 70), 71(12,20) | 99.62 |
| 148 | Pro. | 34(25,34), 39(29,39), 41(30,41), 56(46,56), 75(64,75), 83(72,83), 90(80,90), 95(84,95), 98(87,98), 110(100,110), 112(102,112), 113(104,113), 116(109,116), 128(121,128), 133(124,133), 151(38,59), 153(47,66), 159(105,113), 165(72,144) | 916.937 |

**Table 8** Optimal Routing Results in 69-Bus System

| Search levels | Branch exchange | | | VSI | Critical Voltage | Power loss |
|---|---|---|---|---|---|---|
| | Selected loop network | close | open | | | |
| 1 | - | | | 0.38409 | 0.9092 | 225.0038 |
| 2 | 2 | 73 | 53 | 0.44923 | 0.9245 | 138.9474 |
| 3 | 4 | 72 | 14 | 0.44924 | 0.9245 | 128.2733 |
| 4 | 2 | 53 | 59 | 0.45157 | 0.9263 | 123.0399 |
| 5 | 3 | 74 | 64 | 0.46237 | 0.9414 | 100.7649 |
| 6 | 4 | 14 | 15 | 0.46237 | 0.9414 | 100.6846 |
| 7 | 3 | 64 | 63 | 0.46237 | 0.9414 | 100.6846 |
| 8 | 2 | 59 | 58 | 0.46237 | 0.9414 | 100.6846 |
| 9 | 3 | 63 | 62 | 0.46349 | 0.9428 | 99.6208 |
| Initial tie branch sets obtained from GA | | | | | 70, 71, 72, 73, 74 | |
| Final tie branch sets after BE | | | | | 15, 58, 62, 70, 71 | |
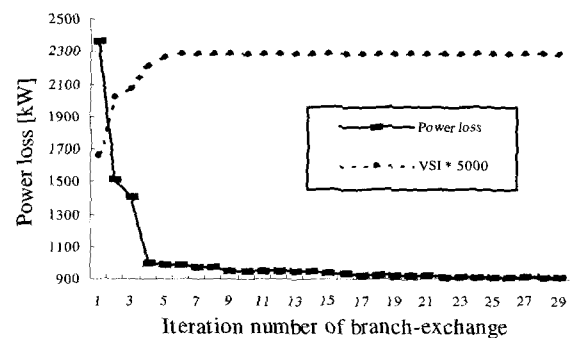


Fig. 7 The optimal routing process of the 148-bus system.

Fig. 8 shows the network topology in the initial step of the 148-bus system. Fig. 9 displays the obtained result in the final step considered as the optimal solution of the system. In both figures, bold lines signify the detected CTP and dotted lines imply opened tie switches. As shown in Fig. 8 and Fig. 9, we can see that the CTP is successively connected in a radial topology. Fig. 10 illustrates that voltage profiles of the 148-bus system are highly improved in all buses following the optimal routing processes.
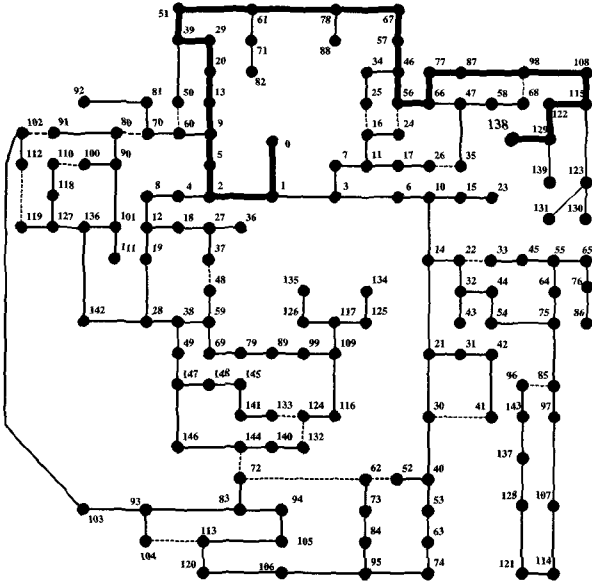
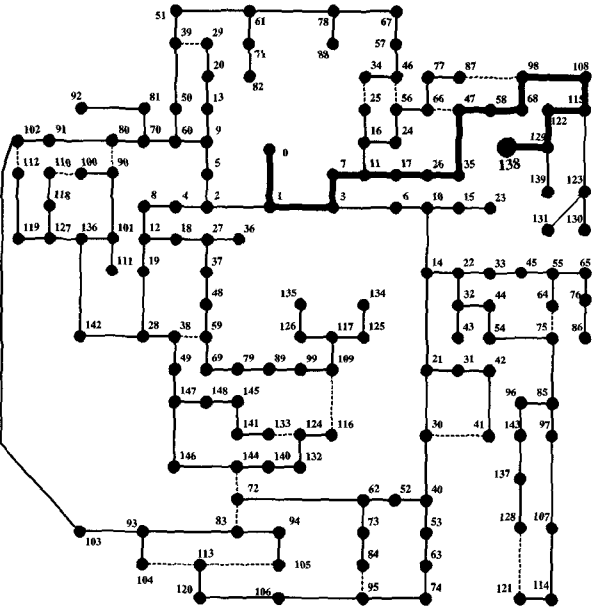**Fig. 8** The CTP in the beginning of the 148-bus system.



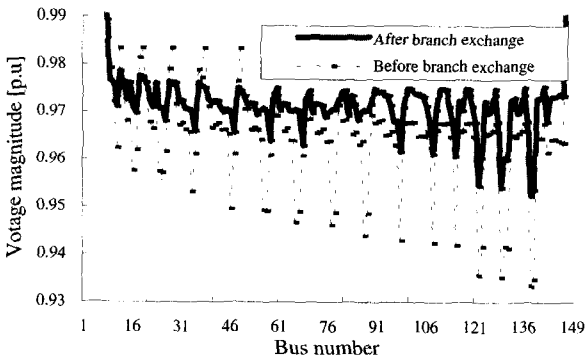**Fig. 9** The CTP in the final stage of the 148-bus system.



**Fig. 10** Comparisons of voltage profiles of the 148-bus system before/after BE.

## 7. Conclusions

This paper has proposed a new optimal routing algorithm to maximize the voltage stability as well as to minimize power loss in radial power systems. The main features of this paper can be summarized as follows:

- An effective VSI has been developed to assess the voltage stability, which is suitable in frequent switching options. As shown in the case studies, the voltage stability of a radial system can be rapidly assessed by the suggested VSI. Furthermore, information of all buses along the CTP and the critical bus can be automatically detected during the BE process. Also, it is assured that the power loss is also minimized when voltage stability is maximized.

- Additionally, the IBE method is proposed to reduce calculation time. The developed IBE method is based on the loss index derived by considering a proportional relationship between real power flow and real power loss. The index can be used as an effective measure to assess the variation of power loss without solving the iterative load flow during the BEs in a loop network. For the estimation of the new tie branch power flow resulting from load transfer during the BEs, the newly derived TBP equation is used. From case studies, it is verified that a TBP can be used within reasonable errors.

- The ORA also has adopted the GA as a global search algorithm. As shown in numerical experiments, it is also assured that the hybrid method is relatively effective in larger-scale systems.

The proposed algorithm has been successfully tested with the IEEE 32-bus, 69-bus systems, and the large-scale KEPCO 148-bus system.

## 8. APPENDIX

### 8.1 Derivation of Det J in (3)

The partial derivative terms in (3) are described as follows:

$$\frac{\partial P_2}{\partial \delta} \frac{\partial Q_2}{\partial V_2} = V_1^2 V_2 (B_{21}^2 \cos^2 \delta - G_{21}^2 \sin^2 \delta)$$

$$+ 2V_1 V_2^2 B_{22} (G_{21} \sin \delta + B_{21} \cos \delta) \qquad (A1\text{-}a)$$

$$\frac{\partial P_2}{\partial V_2} \frac{\partial Q_2}{\partial \delta} = V_1^2 V_2 (G_{21}^2 \cos^2 \delta - B_{21}^2 \sin^2 \delta)$$

$$+ 2V_1 V_2^2 G_{22} (G_{21} \cos \delta + B_{21} \sin \delta) \qquad (A1\text{-}b)$$

Here, G and B imply the real and imaginary parts of bus admittance matrix, respectively. By using (A1), the determinant of the Jacobian matrix in (3) can be finally expressed as follows:

$$Det\ J = V_1^2 V_2 (B_{21}^2 - G_{21}^2) + 2V_1 V_2^2 \cos\delta(B_{21}B_{22} - G_{21}G_{22}) \quad (A2)$$
$$= V_1 V_2 (G_{21}^2 - B_{21}^2)(2V_2 \cos\delta - V_1)$$

## 8.2 Derivation of equivalent impedance in (9)

If a CTP in a radial system is composed of constant power demands as illustrated in Fig. B1, each branch causes line power losses.
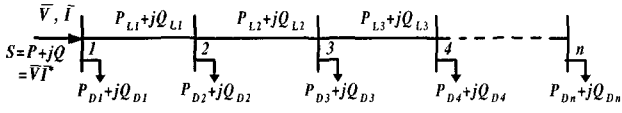


**Fig. B1** Simple network of a critical transmission path.

In Fig. B1, $P_{Li} + jQ_{Li}$ denotes line power loss, and $S = P + jQ$ indicates the injected power flow in the first sending end. From Fig. B1, we can define the equivalent network of the current driving point as shown in Fig. B2.
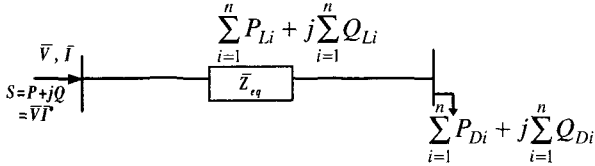


**Fig. B2** Equivalent network of the driving point.

In Fig. B2, we can define the correlative equations as follows:

$$P = \sum_{i=1}^{n} P_{Li} + \sum_{i=1}^{n} P_{Di}, \quad Q = \sum_{i=1}^{n} Q_{Li} + \sum_{i=1}^{n} Q_{Di} \quad (B1\text{-}a)$$

$$\overline{I}^2 \overline{Z}_{eq} = \sum_{i=1}^{n} P_{Li} + j\sum_{i=1}^{n} Q_{Li} \quad (B1\text{-}b)$$

$$\overline{I} = (P - jQ)/\overline{V}^* \quad (B1\text{-}c)$$

By substituting (B1-c) to (B1-b), the following equation can be obtained.

$$[(P^2 + Q^2)/V^2]\overline{Z}_{eq} = \sum_{i=1}^{n} P_{Li} + j\sum_{i=1}^{n} Q_{Li} \quad (B2)$$

In general, the first sending end voltage has unit constant value ($V=1.0$ [p.u]). We can finally derive the

equivalent impedance of the simple network as follows:

$$\overline{Z}_{eq} = r_{eq} + jx_{eq} = (\sum_{i=1}^{n} P_{Li} + j\sum_{i=1}^{n} Q_{Li})/(P^2 + Q^2) \quad (B3)$$

## 8.3 Derivation of Loss Change Index in (14)

To determine the optimum branch in a loop, it requires estimating loss changes after branch exchanges. Since the real power loss of branches before a BE are known, we can estimate the power loss changes in each branch (i) due to a general BE between a tie branch (t) and an adjacent branch (t,con). The derivation of this index starts from the proportional relationship between real power loss and real power flow. First consider the simplified real power loss of the branch flow equation. In (C1), $P_{i,loss}$ and $Q_{i,loss}$ denote the real part loss and reactive part loss of a branch (i) as described in IV. B, respectively.

$$\tilde{P}_L = \sum_{i=1}^{n} r_i (P_i^2 + Q_i^2) = \sum_{i=1}^{n} P_{i,loss} + \sum_{i=1}^{n} Q_{i,loss} \quad (C1)$$

For general branch exchanges, the changes of real part loss and reactive part loss in the branch (i) are described as follows:

$$\Delta P_{i,loss}^L = P_{i,loss}\left\{\frac{(P_i - P_{t,con})^2}{P_i^2} - 1\right\} \quad (i \in L)$$

$$\Delta P_{i,loss}^R = P_{i,loss}\left\{\frac{(P_i + \hat{P}_t)^2}{P_i^2} - 1\right\} \quad (i \in R)$$

(C2-a)

$$\Delta Q_{i,loss}^L = Q_{i,loss}\left\{\frac{(Q_i - Q_{t,con})^2}{Q_i^2} - 1\right\} \quad (i \in L)$$

$$\Delta Q_{i,loss}^R = Q_{i,loss}\left\{\frac{(Q_i + \hat{Q}_t)^2}{Q_i^2} - 1\right\} \quad (i \in R)$$

(C2-b)

After loss changes in each branch have been evaluated, the updated power flow covering all branches can be calculated in both the L-side and R-side as follows:

$$P_i' = P_i - P_{t,con} \quad (i \in L)$$
$$P_i' = P_i + \hat{P}_t \quad (i \in R)$$

(C3-a)

$$Q_i' = Q_i - Q_{t,con} \quad (i \in L)$$
$$Q_i' = Q_i + \hat{Q}_t \quad (i \in R)$$

(C3-b)

Therefore, the total real power changes of a general BE can be calculated in a loop network as in (C4). Using these equations from (C2) to (C4), the total real power changes due to each BE in a loop can be calculated as follows:

$$\Delta P_{loss} = \sum_{i \in L} \Delta P_{i,loss}^{L} + \sum_{i \in R} \Delta P_{i,loss}^{R} + (\hat{P}_t - P_{t,con}) \quad \text{(C4-a)}$$

$$\Delta Q_{loss} = \sum_{i \in L} \Delta Q_{i,loss}^{L} + \sum_{i \in R} \Delta Q_{i,loss}^{R} + (\hat{Q}_t - Q_{t,con}) \quad \text{(C4-b)}$$

## Acknowledgment

## References

[1] P. Ju and X. Y. Zhou, "Dynamic equivalents of distribution systems for voltage stability studies", *IEE Proc.-Gener. Transm. Distrib.*, Vol. 148, No. 1, pp. 49-53, Jan. 2001.

[2] R. Lind and D. Karlsson, "Distribution system modelling for voltage stability studies", *IEEE Transactions on Power Systems*, Vol. 11, No. 4, pp. 1677-1682, Nov. 1996.

[3] J. R. Shin, B. S. Kim, M. S. Chae, and S. A. Sebo, "Improvement of the precise P-V curve considering the effects of voltage dependent load models and transmission losses for voltage stability analysis", *IEE Proc.-Gener. Transm. Distrib.*, Vol. 149, No. 4, pp. 384-388, July 2002.

[4] B. Venkatesh, G. Sadasivam, and M. A. Khan, "A new optimal reactive power scheduling method for loss minimization and voltage stability margin maximization using successive multi-objective fuzzy LP technique", *IEEE Transactions on Power Systems*, Vol. 15, No. 2, pp. 844-851, May 2000.

[5] W. R. Lachs and D. Sutanto, "Different types of voltage instability", *IEEE Transactions on Power Systems*, Vol. 9, No. 2, pp.1126-1134, May 1994.

[6] P. Kundur, *Power system stability and control*, McGraw-Hill, 1993.

[7] F. Gubina and B. Strmcnik, "Voltage collapse proximity index determination using voltage phasors approach", *IEEE Transactions on Power System*, Vol. 10, No. 2, pp. 788-794, May 1995.

[8] A. M. Chebbo, M. R. Irving, and M. J. H. Sterling, "Voltage collapse proximity indicator: behavior and implications", *IEE Proceedings-C*, Vol. 139, No.3, pp. 241-251, May 1992.

[9] G. B. Jasmon and L. H. Lee, "Stability of loadflow techniques for distribution system voltage stability analysis", *IEE Proceedings-C*, Vol. 138, No.6, pp. 479-484, Nov. 1991.

[10] S. Civanlar, J. J. Grainger, and S. H. Lee, "Distribution feeder reconfiguration for loss reduction", *IEEE Transactions on Power Delivery*, Vol. 3, No. 3, pp. 1217-1223, July 1988.

[11] M. E. Baran and F. Wu, "Network reconfiguration in distribution systems for loss reduction and load balancing", *IEEE Transactions on Power Delivery*, Vol. 4, No. 2, pp. 1401-1407, April 1989.

[12] M. E. Baran and F. Wu, "Optimal Sizing of Capacitors Placed on A Radial Distribution System", *IEEE Transactions on Power Delivery*, Vol. 4, No. 1, pp. 735-743, Jan. 1989.

[13] B. S. Kim, J. R. Shin, J. B. Park, M. S. Chae, and S. A. Sebo, "Genetic algorithm based approach to the optimal reactive power dispatch considering the voltage dependency of loads", *Engineering Intelligent Systems for Electrical Engineering and Communications*, Vol. 10, No. 4, pp. 197-203, Dec. 2002.

[14] G. B. Jasmon, "Network reconfiguration for load balancing in distribution networks", *IEE Proc.-Gener. Transm. Distrib.*, Vol. 146, No. 6, pp. 563-567, Nov. 1999.

[15] J. R. Shin, J. C. Kim, and J. O. Kim, "Development of optimal routing techniques in power distribution systems using AI method", Korea Electric Power Corporation, Technical Report, Sep. 2000.

**Byung-Seop Kim**
He received his B.S., M.S., and Ph.D. degrees from Konkuk University in 1994, 1998, and 2002, respectively. Currently, he works as a Research Engineer in the R&D Center of LG Industrial Systems Co. Ltd. (LGIS), Korea. His research interests include the areas of power system optimization, voltage stability analysis, digital substation automation systems, and power market analysis.

**Joong-Rin Shin**
He received his B.S., M.S., and Ph.D. degrees from Seoul National University in 1977, 1984, and 1989, respectively. His major research fields include power system analysis, planning, reliability evaluation, and power system engineering tools. Since 1990, he has been a faculty member in the Dept. of Electrical Engineering, Konkuk University, Seoul, Korea, where he is currently a Professor. From 1977 to 1990, he was an Engineer with the Korea Electric Power Corporation (KEPCO).
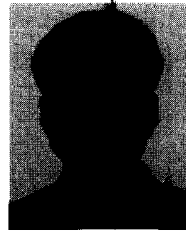
**Yong-Hak Shin**
He received his B.S. and M.S degrees from Hanyang University in 1984, and 1986, respectively. Since 1988, he has worked in the R&D Center of LG Industrial Systems Co. Ltd. (LGIS), Korea and currently is the Head of the IT Solution Research Lab. His main areas of interest are in distributed control systems (DCS), and transmission & distribution information systems for power system control.

**Jong-Bae Park**
He received his B.S., M.S., and Ph.D. degrees from Seoul National University in 1987, 1989, and 1998, respectively. From 1989-1998, he worked as a Researcher at the Korea Electric Power Corporation (KEPCO) and from 1998-2001, he was an Assistant Professor at Anyang University, Korea. Currently, he is an Assistant Professor at Konkuk University, Seoul, Korea. His research interests are in the areas of power system planning, optimization, and economic studies.